A Melanoma Skin Cancer Detection and Classification System Using Deep Transfer Learning

Muhmmad Mateen Yaqoob
Department of Artificial Intelligence & Data Science, National University of Computer and Emerging Sciences (FAST-NUCES), Islamabad, Pakistan
mateen.yaqoob@isb.nu.edu.pk

Sayed Hamidullah
Department of CS, COMSATS University Islamabad, Abbottabad Campus, Abbottabad, KPK, Pakistan
11hamidullah@gmail.com

Razia Manan
Faculty of Arts, Humanities, and Linguistics, IIC University of Technology, Phnom Penh, Cambodia
raziaamir2007@gmail.com

Ali Khalid
School of Computing Sciences, Faculty of Computer Science and Mathematics, Universiti Teknologi MARA, Shah Alam, Selangor, Malaysia
ali.khd.57@icloud.com

Umar Farooq Khattak
School of Information Technology, UNITAR International University, Kelana Jaya, Petaling Jaya, Malaysia
umar.farooq@unitar.my

Muhammad Amir Khan
Faculty of Computer and Mathematical Sciences, Universiti Teknologi MARA, 40450 Shah Alam, Selangor, Malaysia
amirkhan@uitm.edu.my (corresponding author)

Received: 23 October 2025 | Revised: 18 November 2025 and 15 January 2026 | Accepted: 17 January 2026

 DOI: https://doi.org/10.48084/etasr.15730

ABSTRACT

Melanoma is one of the most lethal forms of skin cancer, and early detection is critical for effective treatment and improved survival rates. Traditional diagnosis relies on manual visual inspection of suspicious skin lesions, a process that is time-consuming and subject to human error. This study presents an automated Melanoma Detection System that leverages optimized deep transfer learning to reduce diagnosis time while maintaining high reliability. The proposed method employs a fine-tuned VGG16 model with data augmentation, dropout regularization, and adaptive learning rate optimization, trained on a combined dataset consisting of the Melanoma Skin Cancer Dataset (10,000 images) and the SIIM-ISIC Melanoma Classification dataset. The proposed technique achieve 89% accuracy, 89% precision, 92% recall, and 90.4% F1-score, outperforming baseline CNN and pre-trained architectures. The findings demonstrate that the integration of transfer learning with targeted optimization strategies can significantly improve early detection of melanoma, providing a robust and generalized solution for clinical support.

Keywords-CNN; VGG16; SIIM-ISIC; deep learning; adaptive transfer learning; melanoma skin cancer

I. INTRODUCTION

Throughout a human lifetime, billions of cells in the human body typically grow and die as needed. During this process, the cells continue to produce new cells, while the old or abnormal ones die [1, 2]. Cancer is a disease that can often be effectively treated. There are numerous forms of cancer, which can appear anywhere on the body and are named after specific body parts. For instance, skin cancer starts in the skin, lung cancer starts in the lungs, and breast cancer starts in the breast. If any of the cancer types spread to other parts of the body, it would still be named as the cancer of that body part where it first appeared [3, 4].

Some cancers spread to other body parts, while others remain where they started; some grow quickly, while others develop slowly. Over the past few decades, there has been an increase in both melanoma and non-melanoma skin cancers. Currently, 132,000 cases of melanoma and 2 to 3 million non-melanoma cases of skin cancer are reported annually worldwide [5]. As different types of cancer are being discussed, skin cancer and more specifically, melanoma skin cancer, which is the most lethal kind of skin cancer out of about 200 different types, is targeted. The existing skin cancer diagnosis process of taking the affected area lesion and performing a biopsy is time-consuming and can include human errors in diagnosis. So, there are two main issues: the first is taking too much time to detect, and the second is reducing the human error rate.

Machine learning models can be an optimal solution for both issues. This study trained an adaptive transfer learning model on melanoma skin cancer images (benign, malignant) that consist of different levels of melanoma to achieve a more general model. The major contributions of this study are: (i) presents an optimized transfer learning framework for melanoma detection that enhances the standard VGG16 architecture through selective fine-tuning, redesigned dense layers, and improved regularization, resulting in superior feature discrimination for dermoscopic images; (ii) develops a unified and diversified dataset by systematically integrating the Melanoma Skin Cancer Dataset of 10,000 Images with the SIIM-ISIC dataset, thereby improving model generalization; (iii) introduces an optimization strategy by incorporating learning-rate scheduling, targeted data augmentation, and stability-driven training enhancements.

In [6], an Automated Skin Cancer Detection and Classification method used Cat Swarm Optimization with Deep Learning (ASCDC-CSODL). In this method, Bilateral Filtering (BF) is applied to remove noise, and the U-Net model is used for segmentation. The study in [7] took into consideration the afflicted region in a skin lesion image using a CNN based on ResNet152 to classify the lesions. Using CNN modules such as AlexNet, VGG16, ResNet50, and DenseNet121, the effects of extrinsic items (hairs and a ruler) and image quality (contrast, noise, and blur) on melanoma-identified images were investigated in [8]. This study used data augmentation, trained four modules separately, and examined six datasets. In [9], a transfer-learning method for the diagnosis of skin lesions used three separate feature extractors with comparable input images that were merged in a hybrid CNN classification, used to produce a better depth feature mapping of lesions.

Inception v3 is a deep neural network architecture that uses inception modules with multiple filters to improve feature extraction. This model was trained on a large dataset of skin lesion images, achieving an accuracy of 91% on a test set of 2,032 images [10]. In [11], a deep learning algorithm (VGG16) was used to classify melanoma skin lesions, showing that the model's performance improved with the addition of patient metadata. In [12], an ensemble of ResNet and VGG networks was proposed for skin lesion classification. The models were trained on the ISIC 2018 dataset and achieved an accuracy of 89.1% on a held-out test set. In [13], transfer learning was used with the VGG16 network to classify melanoma skin lesions, but the final fully-connected layer was replaced by a new layer with two output units. The VGG16 network was fine-tuned on a dataset of 2,000 skin lesion images, achieving an accuracy of 82.1%. In [14], an ensemble of Deep Convolutional Neural Networks (DCNNs) for melanoma skin cancer detection achieved an accuracy of 93.45% on a test set of 100 images. In [15], a skin cancer diagnosis model used deep learning algorithms, including Inception-ResNet-v2 and ResNet-101 architectures, achieving an accuracy of 93.5% on a test set of 500 images, outperforming earlier state-of-the-art models by 5.5%.

In [16], an enhanced binary classification method for skin cancer used a CNN and LSTM hybrid strategy. The image of each skin lesion was divided into a tag sequence to capture the temporal dependence using the LSTM, and then the CNN layers were utilized to extract spatial information. In [17], a robust melanoma prediction method used Class Agnostic Activation Maps (CAAM) to address issues related to transformation robustness and variability of skin images. In [18], an ensemble model, consisting of a Vision Transformer (ViT)-based method, a DCNN, and Capsule Networks (CapsNet), was used to detect melanoma skin cancer. This study used the concept of diverse image embeddings for the ensemble method, which was lightweight compared to existing deep learning and ensemble learning methods.

Recently, some studies have utilized transfer learning methods such as DenseNet169 and Resnet-50 to overcome the issue of skin lesion detection and improve model performance [19], transformer-based deep neural networks to capture the spatial dependencies across the skin lesion images without data preprocessing [20], and a federated learning-based methods to improve the melanoma skin cancer classification and privacy of the overall healthcare system [21].

II. THE PROPOSED MODEL

Figure 1 presents a diagram of the proposed system, and Figure 2 presents how its core works. This system aims to be an accurate and reliable system for the detection and classification of melanoma skin cancer. It consists of different stages: a dermoscopic image is uploaded for model prediction, creating a clinical report, consulting a dermatologist for model prediction verification, and providing recommendations.

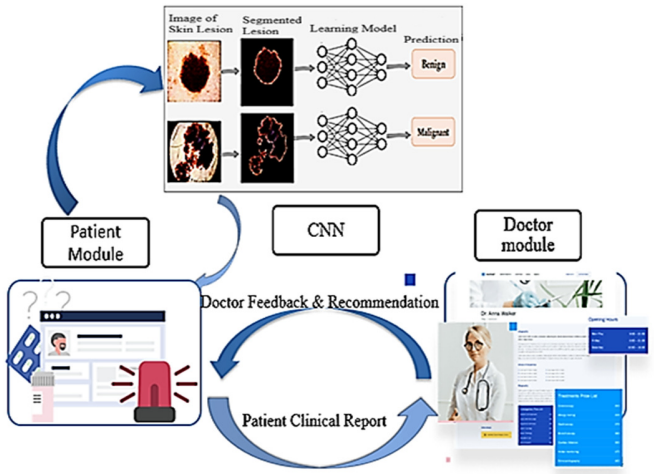

Fig. 1. The proposed architecture.

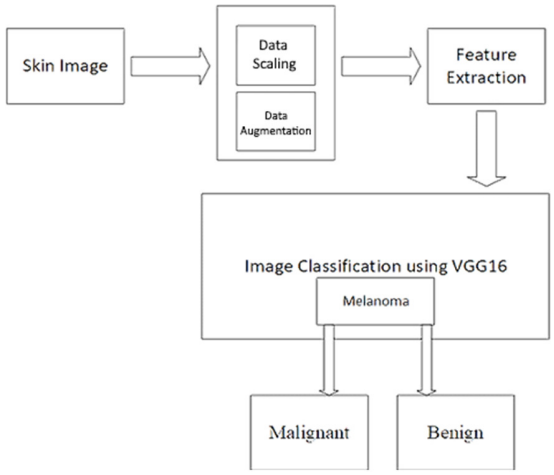

Fig. 2. System block diagram.

A. Mathematical Formulation

Let an input dermoscopic image be represented as:

$$X \in R^{H\times W\times C} \tag{1}$$

where H, W, and C denote the height, width, and number of color channels, respectively. The proposed melanoma classification system processes the image through a series of preprocessing, feature extraction, and visualization steps, as shown in Figure 2, mathematically formulated as follows.

B. Data Scaling

Data scaling is used to ensure that the range of pixel values in the images is normalized to a fixed range of values. This is done to ensure that the model can efficiently learn from the input data. To normalize pixel intensity values, each image X is scaled to the range [0, 1]:

$$[\tilde{X} = \frac{1}{255}X] \tag{2}$$

where 255 is the maximum possible pixel value in an 8-bit image. Scaling ensures numerical stability and prevents vanishing or exploding gradients. Considering a neuron with pre-activation

$$a = w^{\top}x + b \tag{3}$$

the gradient with respect to its weights is given by

$$[\frac{\partial \mathcal{L}}{\partial w} = \frac{\partial \mathcal{L}}{\partial a}\cdot x] \tag{4}$$

If the input is scaled as $x' = \lambda x$, then

$$[\frac{\partial \mathcal{L}}{\partial w'} = \lambda\frac{\partial \mathcal{L}}{\partial w}] \tag{5}$$

indicating that scaling reduces the magnitude of gradient updates by a factor λ, leading to more stable convergence. When the input data is not scaled, it can cause issues like vanishing gradients, which can lead to the model taking a longer time to learn or even getting stuck during training.

C. Data Augmentation

Data augmentation uses novel versions of existing data to fictitiously expand a training dataset. This is accomplished by performing different image transformations, including rotations, zooms, flips, shifts, and shearing. While augmenting data, RandomZoom was set to (0.1), RandomContrast to (0.1), and RandomRotation to (0.2). Let $T_{\phi}(\cdot)$ denote a stochastic image transformation parameterized by ϕ, such as random rotation, zoom, or contrast modification. An augmented image can be expressed as:

$$[\tilde{X} = T_{\phi}(X),\ \phi \sim p(\phi)] \tag{6}$$

where $p(\phi)$ is the probability distribution of transformations. The corresponding augmented empirical risk becomes:

$$[\widehat{R_{\text{aug}}}(\theta) = \frac{1}{N}\sum_{i1}^{N} E_{\phi\sim p(\phi)}\left[\mathcal{L}!\left(f_{\theta}\left(T_{phi}(X_i)\right), y_i\right)\right]] \tag{7}$$

which represents the expected classification loss under all possible transformations. This enforces invariance of the model to rotations, zooms, and contrast variations, thus improving generalization. Then, a random transformation is applied to each image x_i', where the augmentation transformation is defined as:

$$[T(x_i') = \text{RandomRotation}(x_i', 0.2) + \text{RandomZoom}(x_i', 0.1) + \text{RandomContrast}(x_i', 0.1) \tag{8}$$

The augmented dataset $D' = \{(T(x_i'), y_i)\}_{i=1}^{N}$ provides a richer training space, allowing the model to learn robust features invariant to orientation, lighting, and scale variations.

D. Feature Extraction

Feature extraction is performed by the model itself during the training process. The model learns to extract the relevant features from the input data through multiple convolutional and pooling layers. In the VGG16, each layer l extracts hierarchical features using kernels $W_{k,i,j,c}^{(l)}$ as:

$$[A_{u,v,k}^{(l)} = \sigma!\left(\sum_{i1}^{h}\sum_{j1}^{w}\sum_{c1}^{C_{l-1}} W_{k,i,j,c}^{(l)} A_{ui-1,v+j-1,c}^{(l_1)} + b_k^{(l)}\right)] \tag{9}$$

where $\sigma(\cdot)$ is the ReLU activation function. Max-pooling reduces spatial dimensions:

$$[P_{u,v,k} = \max_{(i,j)\in R} A_{i,j,k}^{(l)}] \quad (10)$$

Let $G(X;\theta_{feat})$ represent the feature extractor and $h(\cdot;\ \theta_{head})$ be the classifier head. Then the full model is:

$$[f_\theta(X) = h(G(X;\theta_{feat});\theta_{head})] \quad (11)$$

The overall training objective with L_2-weight regularization is given as:

$$[\min_\theta[\widehat{R_{aug}}(\theta) + \lambda|\theta|_2^2]] \quad (12)$$

and the parameter update rule for iteration t is

$$[\theta_{t+1} = \theta_t - \eta(\nabla_{\theta\mathcal{L}} + 2\lambda\theta_t)] \quad (13)$$

where η is the learning rate and λ is the weight decay coefficient. The categorical cross-entropy loss used for optimization is:

$$[\mathcal{L}(z,y) = -\sum_{k=1}^{K} y_k \log\frac{e^{z_k}}{\sum_{j=1}^{K} e^{z_j}}] \quad (14)$$

where y_k is the one-hot encoded label and z_k the predicted logit for class k.

To visualize which areas have the most contribution in the model's prediction, the Heatmap function is used. The areas of the image with high gradient values are considered to be most important for the prediction, as shown in Figure 3. To interpret model predictions, Gradient-weighted Class Activation Mapping (Grad-CAM) is employed. The importance weight for each feature map is:

$$[\alpha_k^c = \frac{1}{u\,v}\sum_{i=1}^{u}\sum_{j=1}^{v}\frac{\partial z^c}{\partial A_{i,j}^k}] \quad (15)$$

and the corresponding class-discriminative heatmap is:

$$[L_{\text{Grad-CAM}}^c = \text{ReLU!}\,(\textstyle\sum_k \alpha_k^c A^k)] \quad (16)$$

The heatmap $L_{\text{Grad-CAM}}^c$ is then upsampled to the input size and normalized to the range $[0,1]$:

$$[\widehat{L_{\text{Grad-CAM}}^c} = \frac{L_{\text{Grad-CAM}}^c - \min(L_{\text{Grad-CAM}}^c)}{\max(L_{\text{Grad-CAM}}^c) - \min(L_{\text{Grad-CAM}}^c)}] \quad (17)$$

Algorithm 1 describes the overall proposed algorithm.

```
Algorithm 1: Proposed Algorithm for
Melanoma Skin Cancer
Step 1: Data Scaling
  Normalize pixel values for each image x_i
  in the dataset (D) using (2), (3), (4),
  and (5) to scale the pixels into the
  [0,1] range.
Step 2: Data Augmentation
  Apply random transformations to enhance
  dataset diversity using (6), (7), and
  (8). The resulting augmented dataset is
  D' = {(T(x_i'), y_i)}_{i=1}^N
Step 3: Feature Extraction
  Load the pre-trained VGG16 model without
  the top layers. Freeze initial L_f
  convolutional blocks to retain
  pretrained weights. Add new layers:
  Flatten → Dense(256, ReLU) →
  Dropout(0.5) → Dense(128, ReLU) →
  Dense(2, Softmax) using (9), (10), and
  (11).
  Apply regularization using (12).
Step 4: Optimization and Training
  Use Adam optimizer with adaptive
  learning rate decay using (13).
  Compute cross-entropy loss using (14).
  Perform backpropagation and update
  weights for each batch across all
  epochs.
  To interpret model predictions, employ
  Grad-CAM using (15), (16), and (17).
Step 5: Model Output
  After optimization, the final trained
  model is capable of melanoma and non-
  melanoma classification.
```

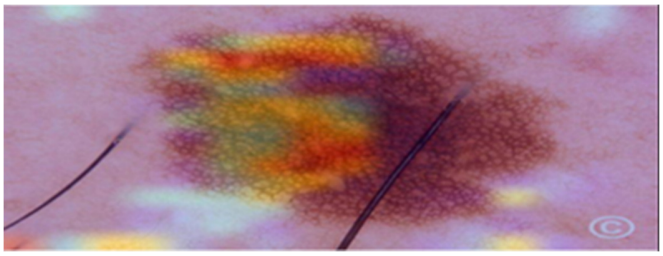

Fig. 3. Uploaded image after the Heatmap function.

III. DATASETS

The Melanoma Skin Cancer Dataset of 10,000 Images [22] was used for training and testing the models, and Table I presents a brief description. In addition, the SIIM-ISIC dataset [23] was used to validate the effectiveness of the proposed skin lesion classification method.

TABLE I. DATASET DESCRIPTION

Attribute	Description
Dataset name	Melanoma Skin Cancer Dataset of 10,000 Images
Domain	Medical Imaging – Dermatology
Total images	10,000 images of skin lesions
Classes/labels	Benign and Malignant (Melanoma)
Image type	RGB images
Image format	JPEG/PNG format
Resolution	Varies between 224×224 and 1024×1024 pixels
Dataset composition	Balanced distribution between benign and malignant categories

IV. RESULTS AND DISCUSSION

The baseline CNN model has six convolutional layers, three max-pooling layers, one flatten layer, and two dense layers, and was trained for twenty epochs. In the VGG16 model [24, 25], there are five max-pooling layers, one average-pooling layer, and four dense layers, trained for twenty epochs. To verify the effectiveness of the proposed method, four baseline algorithms, such as CNN, VGG-16, ResNet50, and MobileNetV2, were

also used. Accuracy, precision, recall, and F1-score were used to assess performance:

$$\text{Accuracy} = \frac{\text{TP+TN}}{\text{TP+TN+FP+FN}}$$

$$\text{Precision} = \frac{\text{TP}}{\text{TP+FP}}$$

$$\text{Recall} = \frac{\text{TP}}{\text{TP+FN}}$$

$$\text{F1} - \text{score} = \frac{2*\text{Precision}*\text{Recall}}{\text{Precision+Recall}}$$

Table II presents a comparative analysis of the classification performance of the deep learning models. The results show a progressive improvement in classification accuracy and performance metrics.

TABLE II. CLASSIFICATION RESULTS AND COMPARISON WITH THE EXISTING METHODS

Model	Accuracy (%)	Precision (%)	Recall (%)	F1-score (%)
CNN	83	82	84	83
VGG-16	85	84	86	85
ResNet50	86	87	88	87
MobileNetV2	87	88	89	88
Proposed (Optimized VGG16 + Adam + LR Decay)	**89**	**89**	**92**	**90.4**

The baseline CNN achieved an accuracy of 83%, but its limitations in precision and recall highlight its inadequate feature representation. VGG-16 offers a modest enhancement with an accuracy of 85%, attributed to its deeper architecture. ResNet50 further enhances classification with an accuracy of 86% and an F1-score of 87%, utilizing residual connections for better feature capture. MobileNetV2 outperforms ResNet50 with an accuracy of 87% and an F1-score of 88%, due to its efficient convolution techniques. The proposed model achieved the best results, with an accuracy of 89%, precision and recall at 89% and 92%, respectively, and a high F1-score of 94%, indicating effective identification, reducing false negatives through advanced optimization strategies.

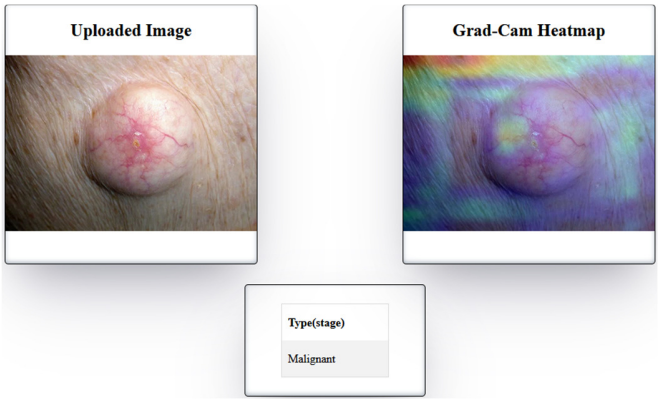

Fig. 4. Model prediction example for malignant.

V. CONCLUSION

The proposed Melanoma Detector System detects benign and malignant melanoma skin lesions. The system is designed to first examine the uploaded image of the patient, whether it is a skin image or not, performing some preprocessing, that is, normalizing the pixel values, and resizing the uploaded image to match the required input size on which the model is trained. After checking the uploaded image, it is passed for prediction. The proposed method was able to achieve better results compared to existing baseline methods. To make the predictions of the Melanoma Detector System more accurate, a Doctor module was added to the system, with the fundamental function to verify the prediction and provide some recommendations based on the patient's case. The doctor module is a single component that distinguishes the proposed system from others already in use for the identification of melanoma skin cancer. In the future, methods for detecting melanoma skin cancer at an early stage can be implemented utilizing machine learning algorithms, transfer learning, and optimization. The effectiveness of the proposed model can also be evaluated using a sizable dataset and an IoT-enabled environment.

REFERENCES

[1] "In brief: How do cancer cells grow and spread?," in *InformedHealth.org*, Cologne, Germany: Institute for Quality and Efficiency in Health Care (IQWiG), 2022.

[2] "Cancer Information for Patients," *CancerCare.com.au*, Aug. 11, 2022. https://cancercare.com.au/patients/cancer-information/.

[3] "What is cancer?,' *World Cancer Day*. https://www.worldcancerday.org/about/what-cancer.

[4] "What Are Advanced and Metastatic Cancers?," *American Cancer Society*. https://www.cancer.org/cancer/understanding-cancer/what-is-cancer/advanced-and-metastatic-cancer.html.

[5] "Radiation: Ultraviolet (UV) radiation and skin cancer," *World Health Organization*. https://www.who.int/news-room/questions-and-answers/item/radiation-ultraviolet-(uv)-radiation-and-skin-cancer.

[6] V. A. Rajendran and S. Shanmugam, "Automated Skin Cancer Detection and Classification using Cat Swarm Optimization with a Deep Learning Model," *Engineering, Technology & Applied Science Research*, vol. 14, no. 1, pp. 12734–12739, Feb. 2024, https://doi.org/10.48084/etasr.6681.

[7] M. F. J. Acosta, L. Y. C. Tovar, M. B. Garcia-Zapirain, and W. S. Percybrooks, "Melanoma diagnosis using deep learning techniques on dermatoscopic images," *BMC Medical Imaging*, vol. 21, no. 1, Dec. 2021, Art. no. 6, https://doi.org/10.1186/s12880-020-00534-8.

[8] B. S. A. Gazioğlu and M. E. Kamaşak, "Effects of objects and image quality on melanoma classification using deep neural networks," *Biomedical Signal Processing and Control*, vol. 67, May 2021, Art. no. 102530, https://doi.org/10.1016/j.bspc.2021.102530.

[9] Md. K. Hasan, T. E. Elahi, Md. A. Alam, T. Jawad, and R. Martí, "DermoExpert: Skin lesion classification using a hybrid convolutional neural network through segmentation, transfer learning, and augmentation," *Informatics in Medicine Unlocked*, vol. 28, 2022, Art. no. 100819, https://doi.org/10.1016/j.imu.2021.100819.

[10] A. Esteva *et al.*, "Dermatologist-level classification of skin cancer with deep neural networks," *Nature*, vol. 542, no. 7639, pp. 115–118, Feb. 2017, https://doi.org/10.1038/nature21056.

[11] T. J. Brinker *et al.*, "Skin Cancer Classification Using Convolutional Neural Networks: Systematic Review," *Journal of Medical Internet Research*, vol. 20, no. 10, Oct. 2018, Art. no. e11936, https://doi.org/10.2196/11936.

[12] K. Shehzad *et al.*, "A Deep-Ensemble-Learning-Based Approach for Skin Cancer Diagnosis," *Electronics*, vol. 12, no. 6, Mar. 2023, Art. no. 1342, https://doi.org/10.3390/electronics12061342.

[13] L. Yu, H. Chen, Q. Dou, J. Qin, and P. A. Heng, "Automated Melanoma Recognition in Dermoscopy Images via Very Deep Residual Networks," *IEEE Transactions on Medical Imaging*, vol. 36, no. 4, pp. 994–1004, Apr. 2017, https://doi.org/10.1109/TMI.2016.2642839.

[14] R. Raza, F. Zulfiqar, S. Tariq, G. B. Anwar, A. B. Sargano, and Z. Habib, "Melanoma Classification from Dermoscopy Images Using Ensemble of Convolutional Neural Networks," *Mathematics*, vol. 10, no. 1, Dec. 2021, Art. no. 26, https://doi.org/10.3390/math10010026.

[15] M. Dildar *et al.*, "Skin Cancer Detection: A Review Using Deep Learning Techniques," *International Journal of Environmental Research and Public Health*, vol. 18, no. 10, May 2021, Art. no. 5479, https://doi.org/10.3390/ijerph18105479.

[16] S. M. M. Abohashish, H. H. Amin, and E. I. Elsedimy, "Enhanced melanoma and non-melanoma skin cancer classification using a hybrid LSTM-CNN model," *Scientific Reports*, vol. 15, no. 1, July 2025, Art. no. 24994, https://doi.org/10.1038/s41598-025-08954-8.

[17] Y. Chu, S. Lee, B. Oh, and S. Yang, "Class-Agnostic Feature-Learning-Based Deep-Learning Model for Robust Melanoma Prediction," *IEEE Journal of Biomedical and Health Informatics*, vol. 29, no. 7, pp. 4946–4955, July 2025, https://doi.org/10.1109/JBHI.2025.3535536.

[18] S. Ghosh, S. Dhar, R. Yoddha, S. Kumar, A. K. Thakur, and N. D. Jana, "Melanoma Skin Cancer Detection Using Ensemble of Machine Learning Models Considering Deep Feature Embeddings," *Procedia Computer Science*, vol. 235, pp. 3007–3015, Jan. 2024, https://doi.org/10.1016/j.procs.2024.04.284.

[19] H. L. Gururaj, N. Manju, A. Nagarjun, V. N. M. Aradhya, and F. Flammini, "DeepSkin: A Deep Learning Approach for Skin Cancer Classification," *IEEE Access*, vol. 11, pp. 50205–50214, 2023, https://doi.org/10.1109/ACCESS.2023.3274848.

[20] M. Gallazzi, S. Biavaschi, A. Bulgheroni, T. M. Gatti, S. Corchs, and I. Gallo, "A Large Dataset to Enhance Skin Cancer Classification With Transformer-Based Deep Neural Networks," *IEEE Access*, vol. 12, pp. 109544–109559, 2024, https://doi.org/10.1109/ACCESS.2024.3439365.

[21] Q. Ul Ain *et al.*, "Privacy-Aware Collaborative Learning for Skin Cancer Prediction," *Diagnostics*, vol. 13, no. 13, July 2023, https://doi.org/10.3390/diagnostics13132264.

[22] "Melanoma Skin Cancer Dataset of 10000 Images." Kaggle, Available: https://www.kaggle.com/datasets/hasnainjaved/melanoma-skin-cancer-dataset-of-10000-images.

[23] "SIIM-ISIC Melanoma Classification." Kaggle, [Online]. Available: https://kaggle.com/siim-isic-melanoma-classification.

[24] G. Rohini, "Everything you need to know about VGG16," *Medium*, Sept. 23, 2021. https://medium.com/@mygreatlearning/everything-you-need-to-know-about-vgg16-7315defb5918.

[25] "Beginners Guide to VGG16 Implementation in Keras," *Built In*. https://builtin.com/machine-learning/vgg16.